Synthesis, Crystal Structure, High-Resolution Optical Spectroscopy, and Extended Hückel Calculations on Cyclometalated [Re(CO)$_4$(ppy)] (ppy = 2-Phenylpyridine)

Frederik W. M. Vanhelmont, Geoffrey F. Strouse,† and Hans U. Güdel*

Institut für anorganische und physikalische Chemie, Universität Bern, Freiestrasse 3, 3000 Bern 9, Switzerland

A. Claudia Stückl

Institut de Chimie Inorganique et Analytique, Université de Fribourg, Pérolles, 1700 Fribourg, Switzerland

Helmut W. Schmalle

Anorganisch-chemisches Institut, Universität Zürich, Winterthurerstrasse 190, 8057 Zürich, Switzerland

Received: September 12, 1996; In Final Form: February 17, 1997[⊗]

The cyclometalated complex [Re(CO)$_4$(ppy)], where ppy$^-$ = 2-phenylpyridine, was synthesized. Its crystal and molecular structure was determined by X-ray diffraction. The lowest energy electronic excitations were studied by high-resolution optical spectroscopy at cryogenic temperature. The first excited state in [Re(CO)$_4$(ppy)] is nominally a triplet ligand-centered state, with 1.8% metal-to-ligand charge transfer character mixed in through spin−orbit coupling. This induces a shortened lifetime (89 μs at 10 K) and the occurrence of metal−ligand vibrations in both absorption and luminescence spectra. The transition moment of the first electronic excitation lies in the molecular plane with a tilt toward the pyridine part of the ppy$^-$ ligand. This is derived from the polarized absorption measurements and confirmed by an extended Hückel calculation. Splittings in the IR absorption bands are resulting from the presence of two crystallographically equivalent complexes in the unit cell which are tilted with respect to each other.

1. Introduction

Hundreds of $(4d)^6$ and $(5d)^6$ complexes with chelating π-accepting ligands have been synthesized. The main scientific interest is in their photophysical and photochemical properties.[1] These are being studied by a variety of physical and chemical techniques. We have concentrated on high-resolution optical absorption and luminescence spectroscopy on single crystals at cryogenic temperatures.[2−4] We have also used the technique of luminescence line narrowing (LLN) on crystalline or glassy matrices at cryogenic temperatures. These techniques often provide significantly more information about energy splittings and vibronic coupling than low-resolution spectra of solutions and glasses. In addition, when the optical measurements on single crystals are combined with the results from X-ray diffraction experiments, we are able to determine the principal directions of the transition moments. This information turns out to be of high value for a proper characterisation of the excited states and an elucidation of the optical transition mechanisms.

More work has been reported on Ru^{2+} complexes than any of the other d^6 ions. The first excited state in $[Ru(bpy)_3]^{2+}$ (bpy = 2,2′-bipyridine) and its many relatives has been classified as metal-to-ligand charge transfer (MLCT).[1a] There is some indirect evidence for a d−d state at slightly higher energy which is assumed to play a role in the photochemistry of these complexes.[5] In $[Os(bpy)_3]^{2+}$ the situation is usually considered to be similar. Due to the higher oscillator strength of the nominally spin-forbidden ^{3}MLCT excitations, there is a stronger tendency toward excitation delocalization than in $[Ru(bpy)_3]^{2+}$.[6]

The first excited state in most of the Rh^{3+}, Ir^{3+}, and Re^+ complexes reported so far has been classified as a ligand-centered (LC) triplet state.[2−4,7] Usually the reduced luminescence lifetime and the higher intensity of the singlet−triplet excitation with respect to the free ligand are taken as a result of some MLCT character which is mixed into the first excited state. In our previous work on mixed-ligand complexes such as $[Rh(bpy)(ppy)_2]^+$ (ppy = 2-phenylpyridine),[2a] we were mainly interested in how the electronic structure and thus the excited state properties are affected when 2,2′-bipyridine is replaced by the 2-phenylpyridine anion. It was possible to identify both the lowest energy ^{3}LC and ^{3}MLCT excitations in the crystal absorption spectrum, and the ^{3}LC absorptions could be assigned to the two ligand types. However, there remained the problem of localization/delocalization of the equivalent transitions on the two ppy$^-$ ligands.

We therefore simplified the situation by studying [Re(CO)$_4$L] complexes with only one chelating π-accepting ligand. In refs 4a and 4b we reported our results on the $[Re(CO)_4(bpy)]^+$ and $[Re(CO)_4(phen)]^+$ complexes (phen = 1,10-phenanthroline). The first excited state is classified as ^{3}LC with a MLCT admixture of approximately 3%. The first transition is polarized along the short ligand axis, i.e. the axis of predominant MLCT intensity. In the present work the effect of cyclometalation on the transition energy, the transition moment, and the degree of LC−MLCT mixing is investigated. To this end we determine the crystal structure, measure polarized single-crystal absorption spectra, and determine the direction of the transition moment. From relative absorption energies and intensities as well as the luminescence lifetime, we obtain an estimate of the LC−MLCT mixing coefficient. LLN spectra provide additional information on the vibronic coupling, in particular the involvement of metal−ligand vibrations in the LC transitions. Extended Hückel (EH) calculations are used to obtain a rough idea about the

* To whom correspondence should be addressed.
† Present address: Materials Research Laboratory, MS G755, LANL, Los Alamos, NM 87545.
⊗ Abstract published in *Advance ACS Abstracts,* April 1, 1997.

S1089-5639(96)02816-2 CCC: $14.00

nature of the relevant orbitals and a prediction of the direction for the transition moment within the molecule.

2. Experimental Section

2.1. Synthesis and Characterization. A synthetic route to [Re(CO)$_4$(ppy)] is described in the literature, but with a rather low yield of 7%.[8] The route described here has a better yield of 27%. The reported calculated percentages for the C and N content in ref 8 are incorrect.

[Re(CO)$_4$(ppy)] was prepared from [Re(CO)$_5$Cl] (Aldrich, 3 mmol), 2-phenylpyridine (Aldrich, vacuum distilled, 3 mmol), and proton sponge (Aldrich, 3 mmol). These starting materials were heated in heptane (Merck, 30 mL) under Ar at 80 °C for 20 h. The yellow solution was filtered and washed several times with a 0.35 M HCl solution and finally with H_2O. The heptane was removed by distillation. The yellow powder thus obtained was dissolved in diisopropyl ether (Fluka). Block and needlelike crystals grew overnight from this solution. From their X-ray powder patterns and elemental analysis, they were identified as two structural modifications of [Re(CO)$_4$(ppy)]. In this paper we report the properties of the blocklike crystals. The whole synthesis was performed under exclusion of light to prevent the formation of possible photoproducts.

Elemental analysis. Calculated: C, 39.82%; H, 1.78%; N, 3.10%; O, 14.14%. Found: C, 40.35%; H, 2.09%; N, 3.17%; O, 14.49% (Ciba-Geigy).

2.2. Crystal Structure Determination. A single crystal with dimensions 0.45 × 0.50 × 0.60 mm was used for the crystal structure determination. Data were collected using an Enraf-Nonius CAD-4 diffractometer. Three standard reflections were measured every 3 h, and three standards were remeasured every 400 reflections to control the orientation of the crystal and the intensity of the reflections. No decay of the intensities was observed during the measuring period. A numerical absorption correction was applied with the MolEN[9a] program system using seven indexed crystal faces. The structure was solved with the Patterson interpretation routine of SHELXS-86.[9b] All non-hydrogen atoms were refined anisotropically. The refinement was performed with all independent F^2 data with the program SHELXL-93.[9c] The H atoms were found by a difference electron density map and refined with isotropic displacement parameters.

2.3. Optical and IR Absorption Spectra. Infrared spectra of a 10^{-4} M solution of [Re(CO)$_4$(ppy)] in CH_2Cl_2 and of crystalline [Re(CO)$_4$(ppy)] in a KBr matrix were measured on a Perkin-Elmer 1720X FTIR spectrophotometer.

The polarized optical absorption spectra of a 10^{-5} M heptane solution and of a single crystal were measured on a Cary 5E spectrophotometer with fixed spectral bandwidths of 1 and 0.07 nm, respectively. The light propagation was perpendicular to the largest crystal face (110). The crystal was cooled in a closed cycle helium cryostat which has been described before.[4]

2.4. Luminescence Spectra. Luminescence experiments were carried out on polycrystalline samples sealed under He in a quartz capillary, on a 10^{-3} M poly(methyl methacrylate) (PMMA) sample or a 10^{-3} M octane solution. The samples were cooled in a double-wall helium gas flow tube as described previously.[9] The samples were excited with an 150 W Oriel Xe lamp, equipped with a Schott UG11 filter to cut off all visible light from the excitation source, with the 457.9 nm line from a Spectra Physics 2045 argon ion laser for the luminescence line narrowed spectra or with a PRA LN250 nitrogen laser for the measurement of the luminescence lifetime. The experimental setup has been described in ref 4.

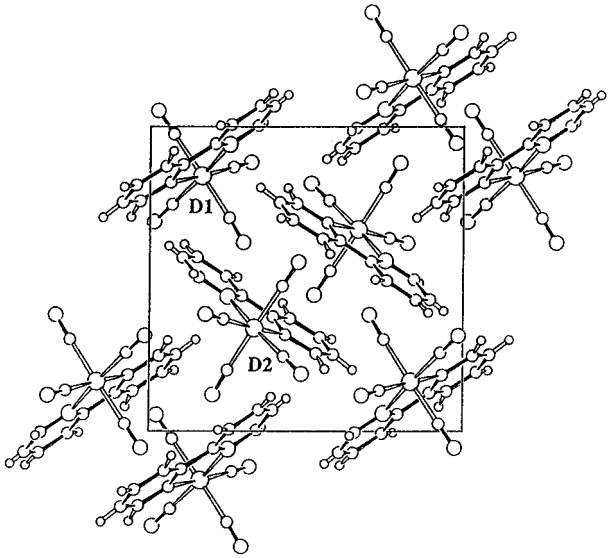

Figure 1. SCHAKAL[29] view of the unit cell of [Re(CO)$_4$(ppy)] along the *a* axis. The molecules labeled D1 and D2 are considered to form a dimer.

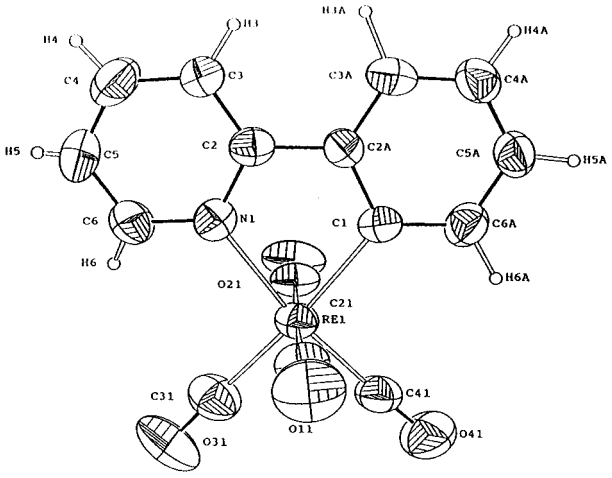

Figure 2. ORTEP plot of [Re(CO)$_4$(ppy)] with the atomic numbering scheme.

3. Results

3.1. Crystal Structure. The largest crystal face of the blocklike crystals of [Re(CO)$_4$(ppy)] has an elongated hexagonal shape, in which the longest edge is the *c* axis. This crystal face is the (110) plane. The space group is $P2(1)/c$. The monoclinic unit cell has the cell constants $a = 10.559(3)$ Å, $b = 11.571(3)$ Å, $c = 12.449(4)$ Å, $\beta = 104.11(3)°$, and $Z = 4$. Crystallographic data are given in Table 1 (Supporting Information). The unit cell viewed along the *a* axis is shown in Figure 1.

The four molecules lie on general equivalent positions in the unit cell. They can be interconverted into each other by an inversion center, a screw axis, or a glide plane. It has been very useful for the interpretation of the infrared absorption spectrum and the determination of the transition moment to consider the unit cell as consisting of two dimers. The members of each dimer are two complexes which are not interconverted by the inversion center (for example, the two molecules with the labels D1 and D2 in Figure 1). They are tilted with respect to each other.

The molecular structure is depicted in Figure 2, with the atom numbering scheme used in the tables. The atomic positional parameters, bond distances, and bond angles are given in Tables

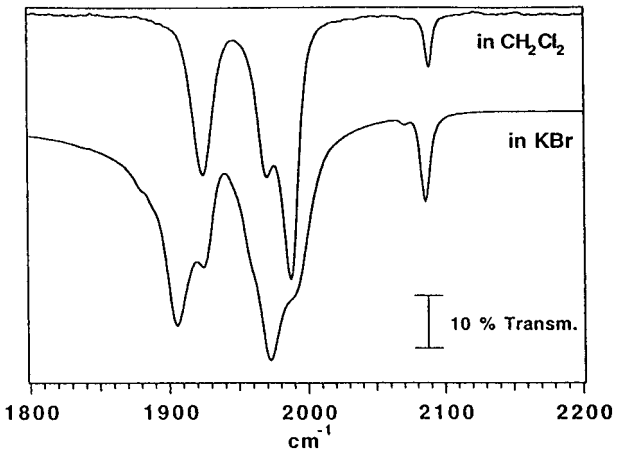

Figure 3. IR spectra of a 10^{-4} M solution of $[Re(CO)_4(ppy)]$ in CH_2Cl_2 and of crystalline $[Re(CO)_4(ppy)]$ in a KBr matrix.

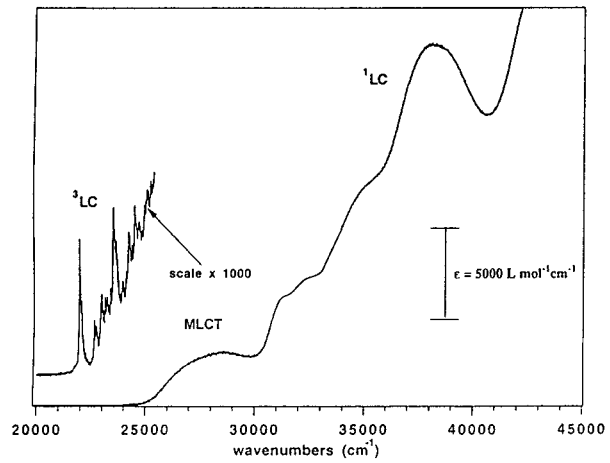

Figure 4. Vis/UV absorption spectrum of a 10^{-5} M solution of $[Re(CO)_4(ppy)]$ in heptane at 295 K supplemented by the unpolarized single-crystal absorption spectrum at 7 K (1000 times enlarged).

2 and 3 of the Supporting Information. In Table 4 of the Supporting Information the positions of the hydrogen atoms with their isotropic displacement parameters are given. The anisotropic displacement parameters for all non-hydrogen atoms are given in the Supporting Information Table 5. The Re−N distance is 0.024 Å longer than the Re−C distance. This difference is smaller than in other ppy$^-$-containing complexes.[2a] The bite angle of ppy$^-$ is 76.2°. The aromatic rings are almost planar: the torsion angle N1−C2−C2A−C1 is 1.1(9)°. The CO ligands have C−Re−C angles ranging from 88.4° to 94.7°. The out-of-plane CO ligands have longer Re−C distances than the in-plane CO ligands (1.914 and 1.941 Å for the in-plane, 1.976 and 1.981 Å for the out-of-plane CO, respectively). All these results are comparable with values found for $[Re(CO)_4(bpy)]^+$ [4a] and $[Re(CO)_4(bpm)]^+$ [7b] (bpm = 2,2′-bipyrimidine).

3.2. Infrared and Optical Absorption Spectra. IR spectra of both a solution and a KBr pellet in the region of the CO stretch vibrations are shown in Figure 3. Four peaks are observed in solution with maxima at 2088, 1988, 1971, and 1925 cm^{-1}. All the bands are split in the spectrum of the crystalline material.

The optical absorption spectrum of a 10^{-5} M heptane solution of $[Re(CO)_4(ppy)]$ is depicted in Figure 4 together with the unpolarized absorption spectrum of crystalline $[Re(CO)_4(ppy)]$. Note that the crystal spectrum is scaled by a factor 1000. The lowest-energy transition could not be seen in solution since it is too weak and inhomogeneously broadened. The higher-energy transitions (above 26 000 cm^{-1}) could not be seen in the crystal spectrum since they are too intense (ϵ > 2500 L mol^{-1} cm^{-1}).

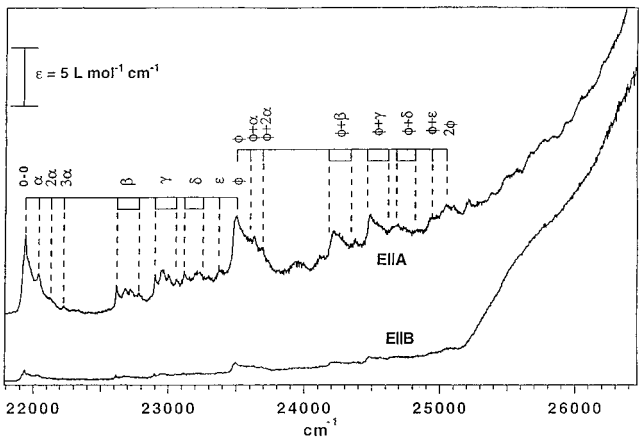

Figure 5. Polarized single-crystal absorption spectra of $[Re(CO)_4(ppy)]$ at 7 K. The light propagation vector is perpendicular to the largest crystal face (110). A and B refer to the extinction directions of the crystal. Fundamental vibrational sidebands and their combination bands for the ϕ = 1563 cm^{-1} mode are indicated.

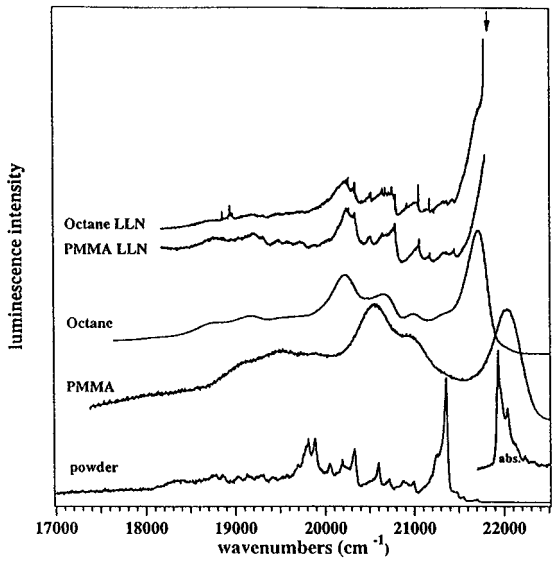

Figure 6. Luminescence spectra of crystalline $[Re(CO)_4(ppy)]$ (bottom) and dissolved in octane and in a PMMA glass (10^{-3} M, middle). The luminescence line narrowed spectra of the same glasses are shown at the top. The arrow indicates the position of the exciting laser. All the spectra were registered at 10 K.

Polarized single crystal absorption spectra are presented in Figure 5. A and B are the optical extinction directions of the crystal in the (110) plane. The angle between A and the *c* axis is 75°. All the absorption bands are more intense for E||A, and the polarization ratio $I(A)/I(B)$ is about six throughout the spectrum. The fine structure is due to vibrational sidebands, overtones, and combination bands of the electronic origin at about 21 940 cm^{-1}. The fundamental vibrations ($\alpha-\phi$) together with the combination bands with the ϕ mode are indicated as well in Figure 5. Similar vibrational energies are measured for the β to ϕ modes in $[Re(CO)_4(ppy)]$ and in $[Re(CO)_4(bpy)]^+$.[4] The α mode on the other hand is found at 99 cm^{-1} here and at 185 cm^{-1} in $[Re(CO)_4(bpy)]^+$.

3.3. Luminescence Spectra. The spectrum of a polycrystalline sample at 10 K is shown at the bottom of Figure 6, with the single crystal absorption origin region included for comparison. The luminescence is red-shifted with respect to the absorption origin, and the spectrum at 10 K exhibits a rich fine structure. At higher temperature the structure fades out, the

band shape changes, and the intensity decreases. This luminescence is obviously dominated by traps. The following two traces in Figure 6 show the $[Re(CO)_4(ppy)]$ luminescence at 10 K in PMMA and octane matrices after broad-band excitation with a xenon lamp. They show the structure typically found in ligand-centered transitions but with considerable inhomogeneous broadening. Their relative displacement by about 300 cm^{-1} reflects the different environments in the two matrices. Excitation with a laser in the spectral region of the first electronic origin (arrow in Figure 6) leads to a sharpening of the features and the occurrence of some very sharp lines on the high-energy side of the vibrational sidebands (see the upper two traces of Figure 6). The sharp lines between 18 800 and 18 900 cm^{-1} in the uppermost trace are C−H stretch Raman lines of octane.

The luminescence decay is single exponential for $[Re(CO)_4(ppy)]$ dissolved in PMMA and octane but not for the crystalline sample. In PMMA the decay time is temperature independent between 10 and 150 K with a value $\tau = 89 \pm 5$ μs. Between 150 and 250 K it drops to 1.2 μs, and above 250 K the luminescence is too weak to be detected. The luminescence intensity drop between 150 and 250 K is similar to the lifetime drop, indicating that nonradiative processes become efficient in this temperature range.

3.4. Extended Hückel Calculations. Fenske−Hall calculations on bpy, ppy^-, and complexes containing these ligands have been published before.[11] However, the authors did not show the spectroscopically relevant orbitals. For this reason we carried out extended Hückel calculations for the free ligand anion ppy^- and for the complex $[Re(CO)_4(ppy)]$ using the CACAO program by Mealli and Proserpio.[12] The positions of the atoms were chosen according to the crystallographic results of $[Re(CO)_4(ppy)]$ (see section 3.1), both for ppy^- and for the complex. The ppy^- rings were considered to be completely planar, thus assuring C_s molecular symmetry, and all the C−H distances were taken as 0.95 Å. The energy level schemes for the free ligand and the complex and a pictorial representation of some relevant orbitals are presented in Figure 7. For the free ligand ppy^- the LUMO is a π*-orbital, whereas the HOMO is an essentially nonbonding σ-orbital. In $[Re(CO)_4(ppy)]$ the LUMO is the same as in the ligand. The HOMO, however, is a π-orbital in the complex. The HOMO in ppy^- drops dramatically in energy between the free ligand and the complex. It forms the Re^+-C^- bond in the complex, and another orbital becomes the HOMO in $[Re(CO)_4(ppy)]$.

All the orbitals of the complex can be related to orbitals of the ligand except the ones indicated with a, b, and c. These are orbitals with a metal d-character of 45, 51, and 48%, respectively. They make up the t_{2g} set of metal orbitals if one considers the complex to have approximate O_h symmetry. The metal d-character in the LUMO is 0% and in the HOMO 2%.

4. Discussion

4.1. Nature of the Lowest Excited State. The bands found in the absorption spectrum of the 10^{-5} M solution of $[Re(CO)_4(ppy)]$ (Figure 4) can be classified in the following way: by comparison with other ppy^--containing complexes[2a,3b,13] and the absorption spectrum of the free ppy,[13] the bands between 30 000 and 40 000 cm^{-1} can be assigned to ^{1}LC transitions. The band between 25 000 and 30 000 cm^{-1} lies in the region where ^{1}MLCT transitions are expected, and we make this assignment. The shoulder in the E||B crystal absorption spectrum around 25 700 cm^{-1} (Figure 5) is assigned to a ^{3}MLCT transition on the basis of its energy and band shape.

The lowest-energy transition found in the single crystal absorption spectrum has a very rich fine structure. It consists of an electronic origin and a series of sidebands, which can be related to vibrations of the ppy^- ligand (Figure 5). By comparison with the single crystal absorption spectrum of $[Re(CO)_4(bpy)]^+$ [4a] and its interpretation, the following tentative assignment of the β to ϕ modes can be made: the β mode is a ring bending mode; γ, δ, ϵ, and ϕ are ring deformation and ligand breathing modes as shown in ref 14. The band shape with the well-resolved and rich vibrational fine structure in the crystal absorption spectrum is strongly indicative of an electronic excitation which is essentially ligand-centered. Similar low-temperature crystal spectra have been measured for $[Rh(bpy)(ppy)_2]PF_6$,[2a] $[Rh(bpy)(thpy)_2]PF_6$[2b] (thpy = 2-(2-thienyl)-pyridine), $[Ir(bpy)(ppy)_2]PF_6$,[3b] $[Ir(bpy)(thpy)_2]PF_6$,[3a] and $[Re(CO)_4(bpy)]PF_6$.[4a] In all these cases the transition was assigned to a ^{3}LC excitation. This assignment is in good accordance with the total absorption intensity. We estimate an oscillator strength $f = 4.2 \times 10^{-5}$ for the lowest-energy transition. In $[Os(bpy)_3]^{2+}$, which also exhibits a great deal of fine structure in the low-temperature absorption spectrum, an oscillator strength of $f = 4 \times 10^{-4}$ is estimated,[15] and a ^{3}MLCT assignment has been made.

Using the formula[3b,16]

$$\tau_{rad} = 1.5 \times 10^4 \left(\frac{1}{f}\right) \frac{(c/\nu)^2}{n((n^2+2)/3)^2} \frac{g_e}{g_g} \qquad (1)$$

we can get an estimate of the radiative lifetime of the first excited state from the measured absorption intensity. In eq 1 f is the oscillator strength, c is the velocity of light, ν is the transition frequency, n is the refractive index, and g_e/g_g are the degeneracies of the excited and ground state, respectively. The refractive index is not known. Choosing a value $n = 1.5$ and taking $f = 4.2 \times 10^{-5}$, we calculate $\tau_{rad} = 74$ μs. The experimental lifetime $\tau = 89 \pm 5$ μs is therefore completely radiative. In $[Os(bpy)_3]^{2+}$, on the other hand, the luminescence lifetime at 4.2 K is $\tau = 10.8$ μs,[17] and in this case the emitting state is considered to be a ^{3}MLCT state.

The phenomenon of luminescence line narrowing is well established in the fluorescence spectroscopy at cryogenic temperatures of aromatic organic molecules diluted into a host crystal or glass matrix.[18] In the complexes $[Rh(bpy)(ppy)_2]^+$, $[Rh(bpy)(thpy)_2]^+$, $[Ir(bpy)(ppy)_2]^+$, $[Ir(bpy)(thpy)_2]^+$,[2,3] we found that the ligand-centered ^{3}LC luminescence could be narrowed to a high degree. In $[Re(CO)_4(bpy)]^+$, on the other hand, only a small fraction of the luminescence could be narrowed,[4b] very similar to the results reported here for the title compound (Figure 6). We do not fully understand all the factors that determine the efficiency of the narrowing process. However, we can take the fact that narrowing does occur as an indication that the transition is essentially ligand centered.

A further confirmation is found in the results of the extended Hückel calculation (Figure 7). The transition from HOMO to LUMO is essentially ligand-centered since the HOMO has only 2% metal character. MLCT transitions from the molecular orbitals designated a, b, and c to the LUMO are also possible, but they are expected at higher energy. Since an extended Hückel calculation takes no account of electron−electron interactions, it is impossible to calculate the energy splitting between the corresponding ^{1}MLCT/^{3}MLCT and ^{1}LC/^{3}LC excitations. But it is well established from experiments that the ^{1}LC/^{3}LC splitting is considerably larger than the ^{1}MLCT/^{3}MLCT splitting. The former is typically larger than 10 000 cm^{-1}, whereas the latter is typically of the order of 2000−4000 cm^{-1}. We thus expect a ^{3}LC first excited state on the basis of the energy level scheme in Figure 7.

4.2. Mixing of LC and MLCT Character. There is ample experimental evidence that the first excited state which we have classified as triplet LC has some singlet character. Its oscillator strength as determined from the absorption spectrum, $f = 4.2 \times 10^{-5}$, is about 4 orders of magnitude bigger than in the free ppy^- ligand, where the lowest singlet−triplet absorption is too weak to be detected.[19,20] Conversely, the luminescence lifetime $\tau = 89 \pm 5$ μs of the title complex is at least 3 orders of magnitude shorter than the lifetime $\tau > 0.1$ s of ppy^-.[20] In $[Ir(bpy)(ppy)_2]^+$ the nominally ppy^- centered ligand excitations have radiative lifetimes of 4.5 μs.[3c] The significantly longer lifetime in the title complex is the result of a much larger energy gap to the relevant MLCT states, resulting in a smaller admixture of MLCT character.

The observation of the α modes in the vibrational sideband structure of the crystal absorption spectrum in Figure 5 is further evidence for the LC−MLCT mixing. The α mode has an energy of 99 cm^{-1}, and we assign it to Re−ligand vibrations. Such modes have been observed in the sidebands of other complexes $[Ir(bpy)(ppy)_2]^+$,[3b] $[Re(CO)_4(bpy)]^+$,[4a] $[Pt(thpy)_2]$,[21] and $[Pd(thpy)_2]$.[21] Their intensity can be taken as a measure of the MLCT character mixed into the first excited state. Also the shoulder about 100 cm^{-1} from the exciting laser line in the LLN spectrum in octane is probably a metal−ligand vibration.

We adopt the model of Komada et al.[22] for an estimate of the LC−MLCT mixing. The authors of ref 22 use second-order perturbation theory to calculate the MLCT character in the lowest-energy ^{3}LC state. The lowest-energy ^{1}MLCT states are considered as the sources of MLCT character, and spin−orbit coupling provides the relevant perturbation. We have used this formalism for estimating the LC−MLCT mixing in the first excited state of other related complexes.[4] Here we refer to refs 22 and 23 and give only a brief summary.

Second-order perturbation theory leads to the following intensity $f_{^3LC}$ which is mixed in by spin−orbit coupling with the spin-allowed ^{1}MLCT excitation:

$$\frac{1}{3}\frac{f_{^3LC}}{f_{^1MLCT}} = \frac{\nu_{^3LC}}{\nu_{^1MLCT}}\left(\frac{\langle {}^3LC|H_{so}|{}^1MLCT\rangle}{h\nu_{^1MLCT} - h\nu_{^3LC}}\right)^2 \qquad (2)$$

with the values of $f_{^3LC}$, $f_{^1MLCT}$, $\nu_{^1MLCT}$, and $\nu_{^3LC}$ taken from the crystal and solution spectra in Figure 4, we obtain a value of 117 cm^{-1} for the matrix element. From this we can calculate the mixing coefficient a in the perturbed ^{3}LC wave function:

$$^3LC_{pert} = \sqrt{1 - a^2}\ {}^3LC_{pure} + a\ {}^1MLCT \qquad (3)$$

The coefficient a is given by

$$a = \frac{\langle {}^3LC|H_{so}|{}^1MLCT\rangle}{E_{^1MLCT} - E_{^3LC}} \qquad (4)$$

which, with the above numbers, is about 1.8%. A value of 3% was estimated for $[Re(CO)_4(bpy)]^+$.[4a]

A result of this MLCT admixture to the ^{3}LC state is a zero-field splitting (zfs) exceeding that of the free ligand. According to ref 22 it can be expressed as follows:

$$\text{zfs} = \langle {}^3LC|H_{so}|{}^1MLCT\rangle^2\left(\frac{1}{(E_{^3MLCT} - E_{^3LC})} - \frac{1}{(E_{^1MLCT} - E_{^3LC})}\right) \qquad (5)$$

The matrix element was evaluated above and the transition energies can be taken from the absorption spectrum. Inserting these values, we get a zfs of 1.5 cm^{-1}. A value of 7.2 cm^{-1} was determined in the related $[Re(CO)_4(bpy)]^+$ complex.[4a] Unfortunately, the zfs is not resolved in our spectra. From the LLN spectra we can give an upper limit of 9 cm^{-1} for the ZFS, which is compatible with the calculated 1.5 cm^{-1}.

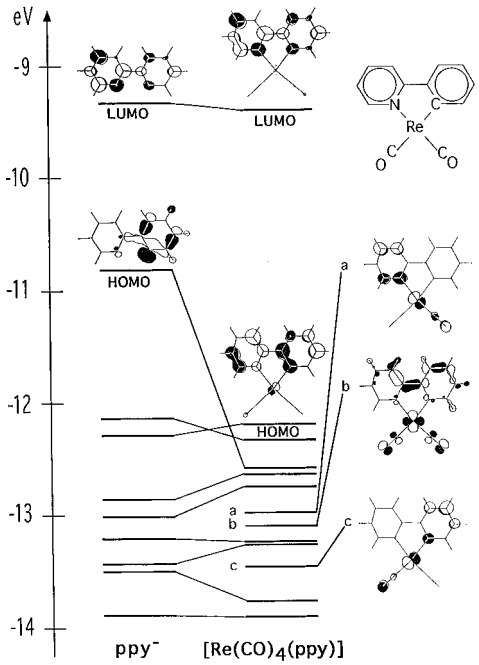

Figure 7. Results of the extended Hückel energy calculations for ppy^- (left) and $[Re(CO)_4(ppy)]$ (middle). The wave functions of the relevant complex orbitals are shown. The contribution of the out-of-plane CO's are not shown to prevent confusion with the contribution of the metal. The orbitals a, b, and c are the nominal "metal orbitals".

4.3. Solid State Effects. In the IR crystal absorption spectrum (Figure 3) we observe energy splittings that are not present in solution and that we ascribe to the particular packing of the molecules in the present crystal structure. Four IR-active C−O stretch vibrations are expected for an isolated $[Re(CO)_4(ppy)]$ molecule of C_s symmetry. This is what we observe in solution; see Figure 3. In the crystal spectrum all the lines are doubled. This is the result of an interaction between the transition dipoles of nearest-neighbor molecules which are tilted with respect to each other.[24] The complexes designated D1 and D2 in Figure 1 are two such molecules. We therefore have to consider the dimer consisting of D1 and D2 as the spectroscopically relevant unit in our crystal. The dimer point symmetry is C_1 and since it contains eight CO groups we expect eight IR-active C−O stretch vibrations as observed. Similar splittings have been found in other crystals.[25] This crystal effect is expected to be biggest in crystals composed of neutral complexes, in which the nearest-neighbor distance is smaller than in a salt.

The presence of this dimer in the unit cell also has consequences on the electronic excitations in the visible part of the spectrum. The interaction of the electronic transition moments of the two molecules leads to a so-called Davydov splitting.[26,27] Using the formulae of ref 26, we estimate an energy splitting of 3 cm^{-1}. This is smaller than the width of the absorption bands and the splitting therefore remains unresolved.

The experimental intensity ratio for the two polarizations I(A)/I(B) in Figure 5 is six. We can use this to determine the molecular transition moment directions $\bar{M}_{D1}$ and $\bar{M}_{D2}$. ($\bar{M}_{D1}$ and $\bar{M}_{D2}$ are the transition moment vectors of D1 and D2, respectively.) Figure 8 shows a projection of D1 and D2 onto

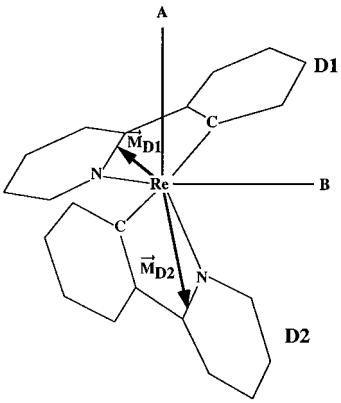

Figure 8. Projection of the complexes D1 and D2 onto the (110) crystal plane with the two Re atoms chosen coincident. A and B are the extinction directions.

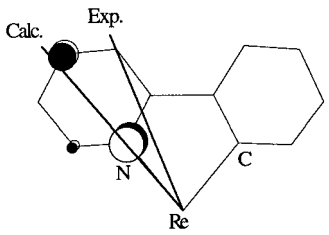

Figure 9. Transitions charge density for the $a \rightarrow$ LUMO excitation according to eq 6: open and full circles. Directions of the experimental and calculated transition moments for the lowest-energy transitions.

the (110) plane, i.e. the crystal face used in the experiment. We assume $\vec{M}_{D1}$ and $\vec{M}_{D2}$ to lie within their respective molecular planes, and by a simple trigonometric exercise using the experimental $I(A)/I(B) = 6$, we obtain the transition moment projections shown in Figure 8. In contrast to [Re(CO)$_4$(bpy)]$^+$ the transition moment is not completely short-axis-polarized.[4a] It is tilted toward the pyridine end of the ppy$^-$ ligand, very similar to the situation in [Rh(ppy)$_2$(bpy)]$^+$.[2a]

A confirmation and interpretation of this tilt is obtained from a calculation of the transition moment using the wave functions of the extended Hückel calculation. In section 4.2 we have identified the lowest-energy MLCT excitations as the principal source of intensity for our nominal ^{3}LC excitation. Possible candidates of one-electron MLCT transitions are a, b, c $\rightarrow$ LUMO transitions. a $\rightarrow$ LUMO is the most likely because it has the lowest energy. b $\rightarrow$ LUMO is ruled out because being $\sigma \rightarrow \pi$ it is symmetry forbidden in first order, and c $\rightarrow$ LUMO is neglected because it lies a few thousand wavenumbers higher in energy. Using the formalism of ref 28 the so-called transition charge density ρ_{kl} can be expressed as follows:

$$\rho_{kl} = -|e|\phi_k\phi_l \qquad (6)$$

where ϕ_k and ϕ_l are the functions of the initial and final orbital, respectively. For the transition a $\rightarrow$ LUMO the result is shown in Figure 9, together with the resulting moment direction. This direction is reasonably close to the experimental one. The tilt toward the pyridine part is overestimated by the calculation.

4.4. Comparison with [Re(CO)$_4$(bpy)]$^+$. One of the main aims of this work was to investigate the effect of cyclometalation on the spectroscopic and excited state properties. The crystal absorption spectrum of both [Re(CO)$_4$(ppy)] and [Re(CO)$_4$(bpy)]-PF$_6$[4a] shows well-resolved fine structure at cryogenic temperatures. In both cases this can be used to derive considerable information about the nature of the first electronic excitation. In both complexes we obtain an admixture MLCT character to the nominally ligand-centered first excited triplet state, brought about by spin−orbit coupling. The relevant coupling matrix element is 261 cm^{-1} in [Re(CO)$_4$(bpy)]PF$_6$ and 117 cm^{-1} in [Re(CO)$_4$(ppy)]. This difference is partially compensated by the energy difference between the ^{3}LC and the ^{1}MLCT states which is larger in [Re(CO)$_4$(bpy)]PF$_6$. The admixture drops from 3% in [Re(CO)$_4$(bpy)]$^+$ to 1.8% in [Re(CO)$_4$(ppy)]. Both ^{3}LC and ^{1}MLCT states are slightly red-shifted in [Re(CO)$_4$-(ppy)].

The transition moment of the first excitation is short-axis-polarized in [Re(CO)$_4$(bpy)]PF$_6$, but in [Re(CO)$_4$(ppy)] it has a long-axis component, tilting toward the pyridine part of the ppy$^-$ ligand. This is the result of an asymmetrical electron distribution in the metal orbitals involved in the MLCT excitations. This, in turn, is clearly a reflection of the different bonding characteristics of the N and C$^-$ ends of the ppy$^-$ ligand. And it can be understood in very simple electrostatic terms: the lowest-energy one-electron excitation from the metal to the ligand avoids the negatively charged phenyl C atom, it is therefore directed toward the N end of the ligand.

Acknowledgment. We thank Naomi Furer for her help in the synthetical work, Marcel Förtsch for indexing the crystal faces, and Thomas Ward, Høgni Weihe, and Andreas Hauser for fruitful discussions. The financial support by the Swiss National Science Foundation is gratefully acknowledged.

Supporting Information Available: Tables 1−5 containing the crystallographic data for [Re(CO)$_4$(ppy)], the atomic coordinates and isotropic displacement parameters, bond lengths and angles, positional parameters for the H atoms, and their isotropic displacement factors and the anisotropic displacement factors for all non-hydrogen atoms (5 pages). Structure factor tables are available upon request from co-author H.W.S. Ordering information is given on any current masthead page.

References and Notes

(1) (a) Juris, A.; Balzani, V.; Barigeletti, F.; Belser, P.; von Zelewsky, A. *Coord. Chem. Rev.* **1988**, *84*, 85. (b) Meyer, T. J. *Acc. Chem. Res.* **1989**, *22*, 163.

(2) (a) Frei, G.; Zilian, A.; Raselli, A.; Güdel, H. U.; Bürgi, H.-B. *Inorg. Chem.* **1992**, *31*, 4766. (b) Colombo, M. G.; Zilian, A.; Güdel, H. U. *J. Am. Chem. Soc.* **1990**, *112*, 4581. (c) Colombo, M. G.; Zilian, A.; Güdel, H. U. *J. Lumin.* **1991**, *48&49*, 549.

(3) (a) Colombo, M. G.; Güdel, H. U. *Inorg. Chem.* **1993**, *32*, 3081. (b) Colombo, M. G.; Hauser, A.; Güdel, H. U. *Inorg. Chem.* **1993**, *32*, 3088. (c) Colombo, M. G.; Hauser, A.; Güdel, H. U. *Top. Curr. Chem.* **1994**, *171*, 144. (d) Colombo, M. G.; Brunold, T. C.; Riedener, T.; Güdel, H. U.; Förtsch, M.; Bürgi, H.-B. *Inorg. Chem.* **1994**, *33* , 545.

(4) (a) Strouse, G. F.; Güdel, H. U.; Bertolasi, V.; Ferretti, V. *Inorg. Chem.* **1995**, *34*, 5578. (b) Strouse, G. F.; Güdel, H. U. *Inorg. Chim. Acta* **1995**, *240*, 453.

(5) Durham, B.; Caspar, J. V.; Nagle, J. K.; Meyer, T. J. *J. Am. Chem. Soc.* **1982**, *104*, 4803.

(6) Riesen, H.; Krausz, E. *Comments Inorg. Chem.* **1995**, *18*, 27.

(7) (a) Spellane, P.; Watts, R. J.; Vogler, A. *Inorg. Chem.* **1993**, *32*, 5633. (b) Shaver, R. J.; Rillema, D. P.; Woods, C. J. *J. Chem. Soc., Chem. Commun.* **1990**, 179.

(8) Bruce, M. I.; Goodall, B. L.; Matsuda, I. *Aust. J. Chem.* **1975**, *28*, 1259.

(9) (a) Fair, C. K. MolEN. An interactive intelligent system for crystal structure analysis. Enraf-Nonius, Delft, The Netherlands, 1990. (b) Sheldrick, G. M. *Acta Crystallogr.* **1990**, *A46*, 467. (c) Sheldrick, G. M. *J. Appl. Crystallogr.*, in press.

(10) Krausz, E.; Tomkins, C.; Adler, H. *J. Phys. E* **1982**, *15*, 8910.

(11) Constable, E. C.; Housecroft, C. E. *Polyhedron* **1990**, *9*, 1939.

(12) Computer Aided Composition of Atomic Orbitals ; original Reference: Mealli, C.; Proserpio, D. *J. Chem. Educ.* **1990**, *67*, 399.

(13) Maestri, M.; Sandrini, D.; Balzani, V.; von Zelewsky, A.; Deuschel-Cornioley, C.; Jolliet, P. *Helv. Chim. Acta* **1988**, *71*, 1053.

(14) (a) Mallick, P. K.; Strommen, D. P.; Kincaid, J. R. *J. Am. Chem. Soc.* **1990**, *112*, 1686. (b) Strommen, D. P.; Mallick, P. K.; Danzer, G. D.; Lumpkin, R. S.; Kincaid, J. R. *J. Phys. Chem.* **1990**, *94*, 1357.

(15) Riesen, H.; Wallace, L.; Krausz, E. *Mol. Phys.* **1996**, *87*, 1299.
(16) Imbusch, G. F. Inorganic Luminescence. In *Luminescence Spectroscopy*; Lumb, M. D., Ed.; Academic Press: London, 1978; pp 1−88.
(17) Lacky, D. E.; Pankuch, B. J.; Crosby, G. A. *J. Phys. Chem.* **1980**, *84*, 2068.
(18) (a) Krausz, E.; Riesen, H. *Comments Inorg. Chem.* **1993**, *14*, 323. (b) Optical Linewidths In *Glasses*; Weber, M. J., Ed. *J. Lumin.* **1987**, *36*, 179−329. (c) Personov, R. I. *Spectroscopy and Excitation Dynamics of Condensed Molecular Systems*; Agranovich, V. M.; Hochstrasser, R. M., Eds.; North-Holland: Amsterdam, 1983; Chapter 10.
(19) Sprouse, S.; King, K. A.; Spellane, P. J.; Watts, R. J. *J. Am. Chem. Soc.* **1984**, *106*, 6647.
(20) Maestri, M.; Sandrini, D.; Balzani, V.; Maeder, U.; von Zelewsky, A. *Inorg. Chem.* **1987**, *26*, 1323.
(21) Yersin, H.; Huber, P. *Coord. Chem. Rev.* **1994**, *132*, 35.
(22) Komada, Y.; Yamauchi, S.; Hirota, N. *J. Phys. Chem.* **1986**, *90*, 6425.
(23) Lever, A. P. B. *Inorganic Electronic Spectroscopy*, 2nd ed.; Elsevier: New York, 1984; pp 176−178.
(24) (a) Cotton, F. A. *Chemical Applications of Group Theory*; John Wiley & Sons: New York, 1990; Chapter 10. (b) Vedder, W.; Hornig, D. F. In *Advances in Spectroscopy*; Thompson, H. W., Ed.; Interscience Publishers: New York, 1961; Vol. II, pp 189−262.
(25) Buttery, H. J.; Keeling, G.; Kettle, S. F. A.; Paul, I.; Stamper, P. J. *J. Chem. Soc. A* **1970**, 471.
(26) Craig, D. P.; Walmsley, S. H. *Excitons in Molecular Crystals*; W. A. Benjamin: New York, 1968; Chapters 1 and 3.
(27) Davydov, A. S. *Theory of Molecular Excitons*; McGraw-Hill Book Company: New York, 1962.
(28) Michl, J.; Thulstrup, E. W. *Spectroscopy with Polarized Light*; Verlag Chemie: New York, 1986; Chapter 2.
(29) Keller, E. SCHAKAL86. A computer program for the graphic representation of molecular and crystallographic models. University of Freiburg, Germany, 1986.